Reactive Thermally Coupled Distillation Sequences: Pareto Front

Erick Yair Miranda-Galindo,[†] Juan Gabriel Segovia-Hernández,*[,†] Salvador Hernández,[†] Claudia Gutiérrez-Antonio,[‡] and Abel Briones-Ramírez[§]

Campus Guanajuato, Departamento de Ingeniería Química, Universidad de Guanajuato, Noria Alta s/n, 36050, Guanajuato, Gto., México, CIATEQ, A.C., Av. del Retablo 150, Col. Fovissste, 76150, Querétaro, Querétaro, México, and Exxerpro Solutions, Av. del Sol 1B Local 4B Plaza Comercial El Sol, 76113, Querétaro, Querétaro, México

Design of reactive distillation sequences is a major computer-aided design challenge. The optimal design of reactive complex distillation systems is a highly nonlinear and multivariable problem, and the objective function used as optimization criterion is generally nonconvex with several local optimums and subject to several constraints. In addition, several attributes for the design of these separation schemes are often conflicting objectives, and the design problem should be represented from a multiple objective perspective. As a result, solving with traditional optimization methods is not reliable because they generally converge to local optimums and often fail to capture the full Pareto optimal front. In this work, we have studied the design of reactive distillation with thermal coupling (using as study case the production of fatty esters), generalizing the use of a multiobjective genetic algorithm with restrictions coupled to Aspen ONE Aspen Plus, previously used in the design and optimization of intensified distillation systems. The results obtained in the Pareto front indicate that the energy consumption of the complex distillation sequence can be reduced significantly by varying operational conditions. Trends in the energy consumption, total annual cost, and greenhouse gas emissions of the thermally coupled reactive distillation sequences can be obtained.

1. Introduction

The design of new processes in chemical engineering takes into account policies of process intensification, which can be defined as any chemical engineering development that leads to a substantially smaller, cleaner, and more energy-efficient technology,[1] for example, minimization of energy consumption, which is associated with lower greenhouse gas emissions, miniaturization of process equipment, multipurpose equipment, safety operations, and others.[2]

One of the most common examples of the process intensification field is the reactive distillation, where the integration of reaction and separation is performed. According to Harmsen,[3] in all the cases where reactive distillation is used, variable cost, capital expenditure, and energy requirement are reduced by 20% or more, when compared to the classic setup of a reactor followed by distillation. These significant savings have motivated the development of optimization strategies to get optimal designs of reactive distillation columns;[4−9] this is not an easy task, because design issues for reactive distillation systems are significantly more complex than those involved in ordinary distillation.[4] Nevertheless, we have to remember that in the classical reactive distillation, just conventional distillation columns are considered, which are well-known by their low thermodynamic efficiency. Thereby, the process of reactive distillation can be intensified even more if thermally coupled distillation is employed. Therefore, in reactive thermally coupled distillation, we can expect additional energy savings and also an optimal design problem even more complex, due to the reactions issues themselves and the complex design of thermally coupled distillation sequences.

Thermally coupled distillation sequences, TCDS, are distillation columns linked between them through vapor and liquid interconnection streams; these interconnection streams allow avoiding the use of condensers or reboilers. In this way, important reductions in energy consumption and also in capital costs can be expected. The simplest configurations of the TCDS, for the separation of ternary mixtures, are direct thermally coupled sequence, indirect thermally coupled sequence, and Petlyuk sequence (usually implemented as a Kaibel column), Figure 1.

As can be seen in Figure 1, the interconnection streams of the TCDS have an important role; through proper selection of the flow values, significant energy savings can be obtained (and, consequently, reductions in CO_2 emissions) over the energy consumption of conventional distillation sequences. There is a considerable amount of literature analyzing the relative advantages of TCDS for ternary separations with equilibrium and nonequilibrium stage models.[10−18] These studies have shown that thermally coupled distillation schemes are typically capable of achieving 30% energy savings over conventional schemes.

Recently, several studies have reported the possibility of implementing the process of reactive distillation in thermally coupled distillation sequences. In these conditions, it is possible to combine the kindness of reactive distillation and the energy savings widely reported for systems with thermal coupling.[19−22] These works show that it is feasible to perform a reaction and separation in a thermally coupled distillation sequence, in particular, in dividing wall columns.

It is clear that reactive thermally coupled distillation sequences, RTCDS, can be used in cases where, at least, the unreacted compounds and products integrated a ternary mixture. This, a priori, defines a subset of processes of reaction−separation that can be implemented in these schemes. For instance, a reaction of the type:

$$A + B \rightarrow C \tag{1}$$

where reactive A or B disappears completely is not suitable for their implementation in a reactive thermally coupled distillation sequence. However, in most of the industrial cases, the reactive processes involve several reactions that occur simultaneously,

* To whom correspondence should be addressed. Tel.: +52 (473) 732-0006 ext. 8142. E-mail: gsegovia@quijote.ugto.mx.
[†] Universidad de Guanajuato.
[‡] CIATEQ.
[§] Exxerpro Solutions.

10.1021/ie101290t
Published on Web 12/13/2010

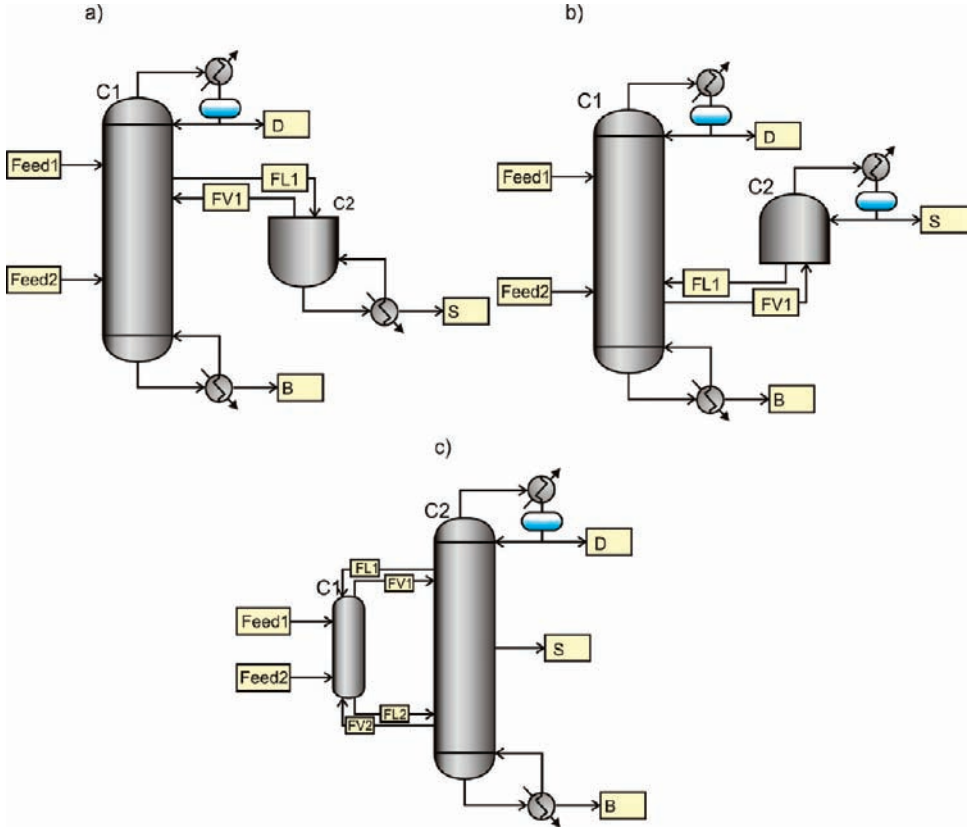

Figure 1. Thermally coupled reactive distillation sequences: (a) direct (STADR), (b) indirect (STAIR), and (c) Petlyuk (PETR).

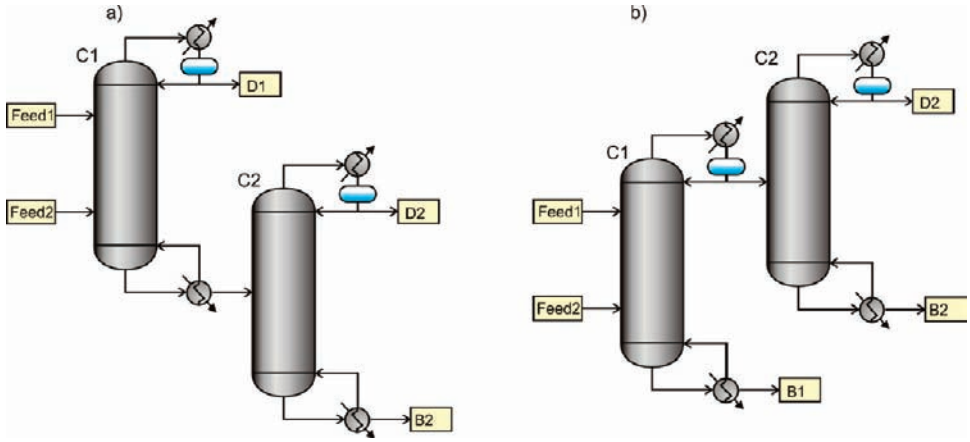

Figure 2. Conventional reactive distillation sequences: (a) direct (SDCR), and (b) indirect (SICR).

and, also, they are in competence. The kinetics, selectivity, and simultaneity of the industrial reactions are varied and, also, the configurations of the TCDS. Therefore, it is difficult to know beforehand what configuration is the most adequate for a certain type of reaction; even knowing which one is the best configuration, to our knowledge, no formal design methodologies have been developed for this kind of sequences.

So, in this work, we analyze three thermally coupled configurations, direct thermally coupled distillation sequence, indirect thermally coupled distillation sequence, and Petlyuk sequence, Figure 1, and also two reactive conventional schemes, direct and indirect reactive distillation sequences, Figure 2. In these systems, a reaction of the following type is performing:

$$A + B \rightarrow C + D \tag{2}$$

We select this kind of reaction because it is the simplest case where a ternary mixture can be integrated, considering that one reactive completely disappears. To analyze the best scheme for this type of reaction, we obtain Pareto fronts of the three reactive thermally coupled and two conventional distillation sequences; the Pareto fronts were generated with a multiobjective genetic algorithm with constraints,[23] which is coupled to Aspen Plus. In this way, we can analyze the energy consumptions, configurations, size of the reactive section, and other valuable information in the optimal designs of these sequences. Results show interesting data about the best schemes for this type of reaction, and also about the design variables of these schemes.

2. Problem Statement

Fatty esters are important fine chemicals used in the manufacturing of cosmetics, detergents, and surfactants. Particularly, methyl ester could play a significant role in the future as a major component of biodiesel fuels.[24] Next, the esterification reaction

Table 1. Kinetic Parameters for the Pseudohomogeneous Kinetic Model of the Esterification Reaction

reaction	k_i^o (mol/g·s)	$E_{A,i}$ (kJ/mol)
esterification	9.1164×10^5	68.71
hydrolysis	1.4998×10^4	64.66

to generate biodiesel can be conceptually represented by the following equation:

$$\text{alcohol} + \text{fatty acid} \leftrightarrow \text{ester} + \text{water} \quad (3)$$

Particularly, the esterification of methanol and lauric acid is studied using the reactive thermally coupled, Figure 1, and reactive conventional, Figure 2, distillation sequences. In this reaction, lauric acid is the limiting reactive, so a mixture comprised of methanol, water, and the ester (biodiesel) is integrated. The equilibrium of this reaction can be favored if the products are removed as the reaction proceeds. Because of this, we are considering that the reaction just occurs in a section of the first distillation column, and not in the second one.

An additional problem may present itself, depending on the acid and the alcohol used, as binary or ternary homogeneous azeotropes can be formed in the reactive system. For highly nonideal systems, heterogeneous azeotropes can be formed.[24] These key factors must be considered in order to select the appropriate thermodynamic model when the system is studied with process simulators. For this class of reactive systems, thermodynamic models such as NRTL, UNIFAC, or UNIQUAC can be used to calculate vapor−liquid or vapor−liquid−liquid equilibrium. For this study (esterification of methanol and lauric acid), we selected the UNIFAC model.

The systems include two feed streams: the first is lauric acid with a flow of 45.4 kmol/h as saturated liquid at 1.5 bar, and the second is methanol with a flow of 54.48 kmol/h as saturated vapor at 1.5 bar. The design objective is a process for high-purity fatty ester, over 99.9% mass fraction, suitable for applications in cosmetics, detergents, surfactants, or biodiesel application. It is important to highlight that this equilibrium reaction is usually catalyzed using sulfuric acid or *p*-toluensulfonic acid. The kinetic model (see Table 1) reported in Steinigeweg and Gmehling[25] was used.

3. Optimization Problem

The intensified process, reaction and distillation, is going to be performed in thermally coupled and conventional schemes. Next, the optimization problem is established for each sequence, considering the objectives, constraints, and variables included.

For all schemes presented here, methanol is fed in excess to the reaction that is performed with lauric acid. We consider a complete conversion of the lauric acid, and that excess methanol is only obtained as a product. Considering this, we performed the material balances for the products of the reaction. Thereby, the recoveries and mass purities of unreacted methanol and water are calculated with respect to the results of the material balances and are set at 98%. For the ester, we specify 99.9% for the mass purity and the recovery. It is worth mentioning that the conversion of the reaction is not an optimization objective itself; however, we specify the recoveries of the unreacted compound, methanol, and of the principal product, ester, as constraints of the problem. Thereby, indirectly, the conversion is considered as an objective.

Reactive Direct Conventional Sequence. In the reactive direct conventional distillation, SDCR, sequence there are five objectives to minimize: total number of stages and heat duty in each column, along with the size of the reactive section in the first column, see Table 2. The minimization of these objectives is subject to the required recoveries and purities in each product stream:

Table 2. Objectives To Be Simultaneously Minimized To Generate the Pareto Fronts of Each Reactive Scheme

	direct conventional	indirect conventional	direct thermally coupled	indirect thermally coupled	Petlyuk
number of stages in column C1, N_{C1}	X	X	X	X	X
number of stages in column C2, N_{C2}	X	X	X	X	X
heat duty in column C1, Q_{C1}	X	X	X	X	
heat duty in column C2, Q_{C2}	X	X		X	X
size of the reactive section in column C1, $N_{R,C1}$	X	X	X	X	X

Table 3. Manipulated Variables To Generate the Pareto Fronts of Each Reactive Scheme

	direct conventional	indirect conventional	direct thermally coupled	indirect thermally coupled	Petlyuk
reflux ratio in column C1, R_{C1}	X	X	X	X	
feed stage of reactive 1 in column C1, $N_{F1,C1}$	X	X	X	X	X
feed stage of reactive 2 in column C1, $N_{F2,C1}$	X	X	X	X	X
number of stages in column C1, N_{C1}	X	X	X	X	X
reflux ratio in column C2, R_{C2}	X	X			X
feed stage in column C2, $N_{F,C2}$	X	X			
number of stages in column C2, N_{C2}	X	X	X	X	X
first reactive stage in column C1, $N_{R1,C1}$	X	X	X	X	X
last reactive stage in column C1, $N_{R2,C1}$	X	X	X	X	X
distillate streamflow of column C1	D1		D	D	D
distillate streamflow of column C2	D2	D2	S		
bottoms streamflow of column C2		B2		S	
side streamflow of column C2					S
product stage of liquid interconnection flow FL in column Ci, $N_{FL,Ci}$				$N_{FL1,C1}$	$N_{FL1,C2}$
feed stage of vapor interconnection flow FV in column Ci, $N_{FV,Ci}$				$N_{FV1,C1}$	$N_{FV1,C2}$
vapor interconnection flow, FV			FV1		FV2
feed stage of liquid interconnection flow FL in column Ci, $N_{FL1,Ci}$			$N_{FL1,C1}$		$N_{FL2,C2}$
product stage of vapor interconnection flow FV in column Ci, $N_{FV,Ci}$			$N_{FV1,C1}$		$N_{FV2,C2}$
liquid interconnection flow, FL				FL1	FL1
product stage of the side stream S in column Ci, $N_{S,Ci}$					$N_{S,C2}$
total	11	11	12	12	16

$$\min(Q_{C1}, Q_{C2}, N_{C1}, N_{C2}, N_{R,C1}) \quad \text{subject to} \quad \vec{y}_m \geq \vec{x}_m \tag{4}$$

where Q_{Ci} is the heat duty of the column Ci, N_{Ci} is the number of stages of the column Ci, $N_{R,C1}$ is the size of the reactive section in the first column, and y_m and x_m are vectors of obtained and required purities for the m components, respectively. This minimization implies the manipulation of 11 variables as continuous as integer, Table 3. Note that because the product streams flows are manipulated, the recoveries of the key components in each product stream must be included as a restriction.

Reactive Indirect Conventional Sequence. In the reactive indirect conventional distillation sequence, SICR, there are also five objectives to minimize: total number of stages and heat duty in each column, along with the size of the reactive section in the first column, see Table 2. The minimization of these objectives is subject to the required recoveries and purities in each product stream:

$$\min(Q_{C1}, Q_{C2}, N_{C1}, N_{C2}, N_{R,C1}) \quad \text{subject to} \quad \vec{y}_m \geq \vec{x}_m \tag{5}$$

where Q_{Ci} is the heat duty of the column Ci, N_{Ci} is the number of stages of the column Ci, $N_{R,C1}$ is the size of the reactive section in the first column, and y_m and x_m are vectors of obtained and required purities for the m components, respectively. This minimization implies the manipulation of 11 variables as continuous as integer, Table 3. Note that the difference between the direct and indirect conventional sequences lies on the manipulated product flows: two distillates in the direct case, and one distillate and one bottom for the indirect sequence.

Reactive Direct Thermally Coupled Sequence. On the other hand, for the reactive direct thermally coupled distillation sequence, STADR, there are four objectives to minimize: total number of stages in each column, the size of the reactive section in the first column, and the heat duty of the sequence, see Table 2. The minimization problem can be expressed as:

$$\min(Q_{C1}, N_{C1}, N_{C2}, N_{R,C1}) \quad \text{subject to} \quad \vec{y}_m \geq \vec{x}_m \tag{6}$$

where Q_{Ci} is the heat duty of the column Ci, N_{Ci} is the number of stages of the column Ci, $N_{R,C1}$ is the size of the reactive section in the first column, and y_m and x_m are vectors of obtained and required purities for the m components, respectively. This minimization implies the manipulation of 12 variables as continuous as integer, Table 3.

Reactive Indirect Thermally Coupled Sequence. In the case of the reactive indirect thermally coupled sequence, STAIR, five objectives are minimized: total number of stages in each column, the size of the reactive section in the first column, and the heat duty of the sequence, see Table 2. The minimization problem can be formulated as follows:

$$\min(Q_{C1}, Q_{C2}, N_{C1}, N_{C2}, N_{R,C1}) \quad \text{subject to} \quad \vec{y}_m \geq \vec{x}_m \tag{7}$$

where Q_{Ci} is the heat duty of the column Ci, N_{Ci} is the number of stages of the column Ci, $N_{R,C1}$ is the size of the reactive section in the first column, and y_m and x_m are vectors of obtained and required purities for the m components, respectively; it is important to note that for the indirect reactive sequence there is an additional heat duty to minimize.

The optimization of this scheme also implies the manipulation of 12 variables as continuous as integer, Table 3.

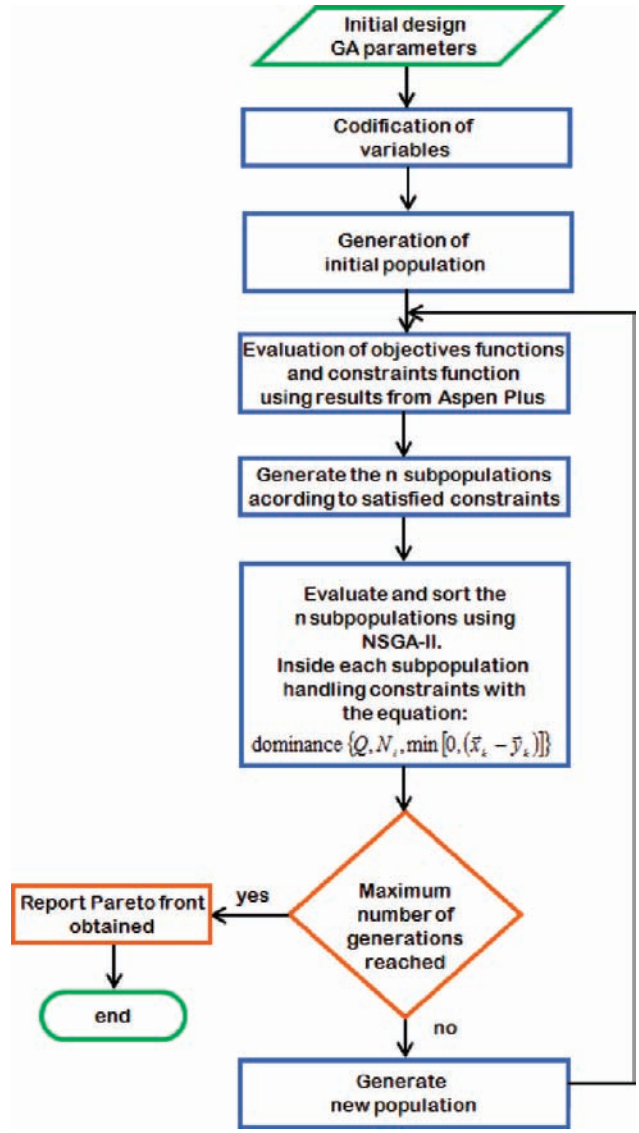

Figure 3. Flowchart of the multiobjective genetic algorithm with constraints coupled to Aspen ONE Aspen Plus.

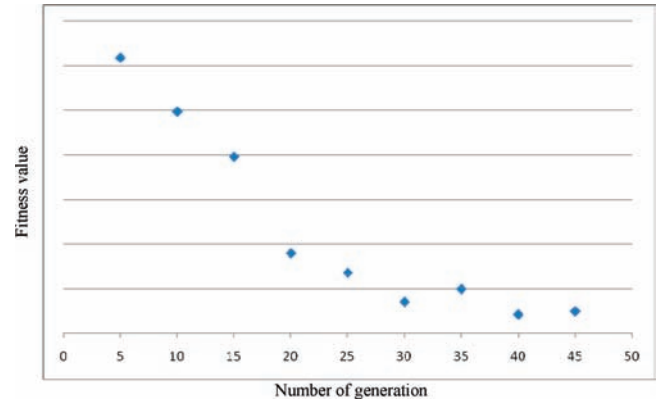

Figure 4. Convergence plot of the reactive direct conventional sequence for 2000 individuals.

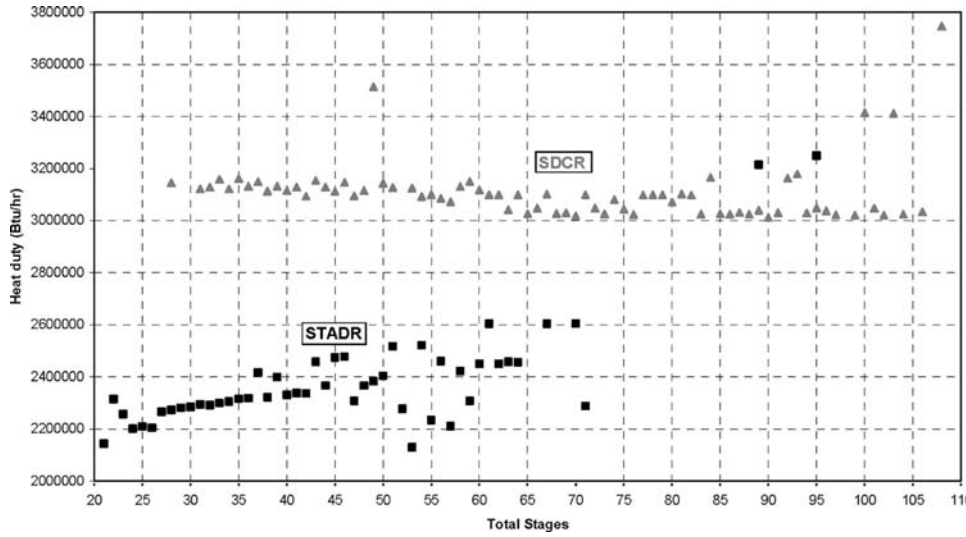

Figure 5. Total number of stages versus energy consumption of thermally coupled, STADR, and conventional, SDCR, reactive direct sequences.

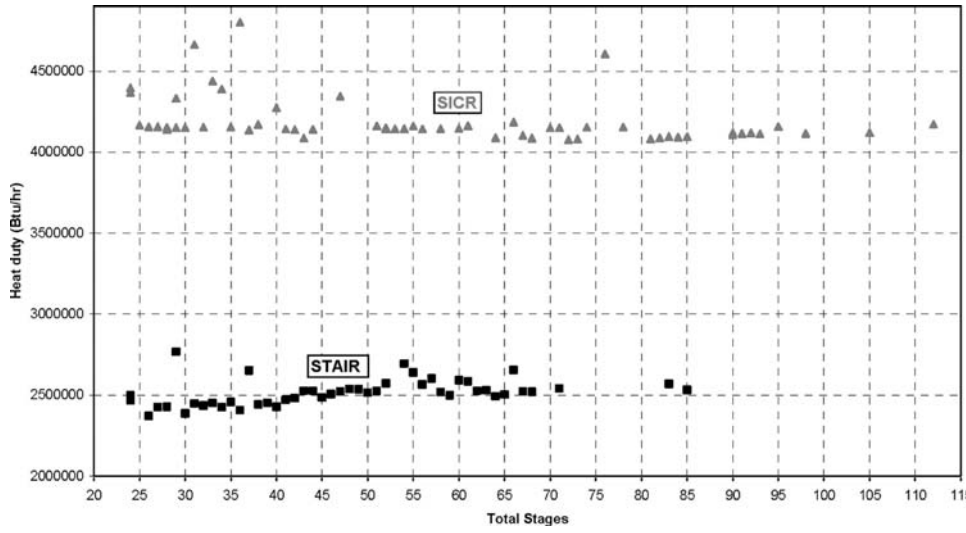

Figure 6. Total number of stages versus energy consumption of thermally coupled, STAIR, and conventional, SICR, reactive indirect sequences.

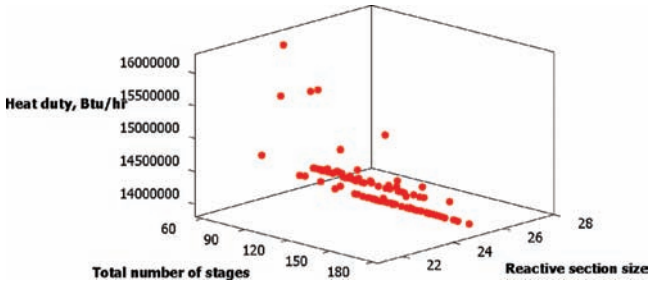

Figure 7. Total number of stages versus energy consumption and size of the reactive section of Petlyuk sequences, PETR.

Reactive Petlyuk Sequence. Finally, the minimization of four objectives is performed for the reactive Petlyuk sequence, PETR: total number of stages in each column, the size of the reactive section in the first column, and the heat duty of the sequence, see Table 2. The minimization problem can be formulated as follows:

$$\begin{aligned} &\min(Q_{C2}, N_{C1}, N_{C2}, N_{R,C1}) \\ &\text{subject to} \\ &\vec{y}_m \geq \vec{x}_m \end{aligned} \tag{8}$$

where Q_{Ci} is the heat duty of the column Ci, N_{Ci} is the number of stages of the column Ci, $N_{R,C1}$ is the size of the reactive section in the first column, and y_m and x_m are vectors of obtained and required purities for the m components, respectively; it is important to note that for the reactive Petlyuk sequence there is just one heat duty to minimize. The optimization task implies the manipulation of 16 variables as continuous as integer, Table 3. In this case, we allow that each interconnection stream can be located in a different stage in the main column; in other words, four interconnection stream stages are allowed.

4. Multiobjective Stochastic Strategy

The optimal designs of these schemes represent a multiobjective and constrained problem, as was pointed in section 3. When multiple objectives are considered in an optimization problem, one solution is not desirable. Instead of that, a set of optimal designs that represents the best trade-off between the considered objectives is desirable. This set of optimal designs integrated a Pareto front, which is defined below.

We can say that a point in the search space is considered to be the Pareto optimum if there is no feasible vector that can decrease the value of one objective without simultaneously increasing the value of another objective, in the case of

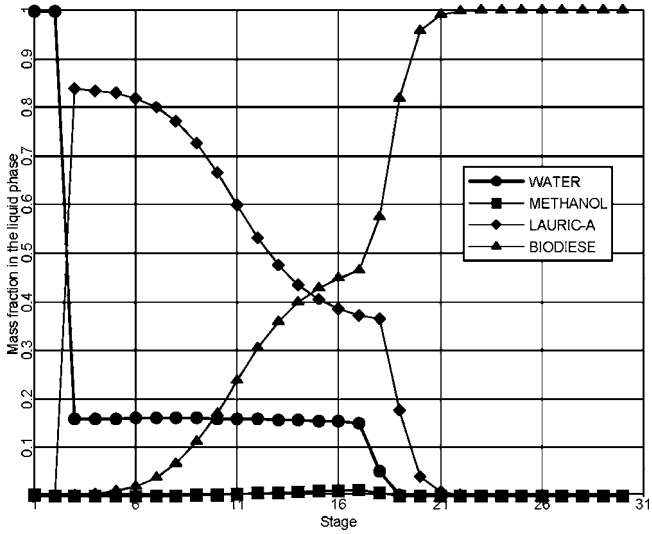

Figure 8. Composition profiles in liquid phase, direct reactive thermally coupled sequence.

minimization. Now, we define that $\vec{x}$ dominates $\vec{y}$ when $f(\vec{x}) < f(\vec{y})$, if $Y \subseteq \mathscr{S}$ and $\vec{y} \in Y$; if no $\vec{x} \in Y$ dominates $\vec{y}$, we say that $\vec{y}$ is not dominated with respect to Y. The set of solutions not dominated that are optimums of Pareto is the Pareto front.

Thus, the Pareto front represents all optimal designs, from minimum number of stages (total reflux ratio) to minimum reflux ratio (infinite number of stages), and all designs between these extremes. This set of optimal solutions allows the engineer to choose a good compromise between the two goals by picking a point somewhere along the Pareto front. Once that Pareto fronts are obtained, an analysis is realized on the resulting data, looking for some tendencies in the variables of interest of these sequences, and also to find the best scheme for this particular reaction.

In particular, the optimal design of reactive distillation systems, as complex as conventional, is a highly nonlinear and multivariable problem, with the presence of both continuous and discontinuous design variables; also, the objectives functions used as optimization criterion are generally nonconvex with several local optimums and subject to several constraints. Also, this optimal problem is a multiobjective problem, because variables as number of stages, size of the reactive section, and heat duty of the sequence are in competition between each other.

Next, to optimize the reactive sequences, we used a multiobjective genetic algorithm with constraints[23] coupled to Aspen ONE Aspen Plus. The stochastic strategy is based on NSGA-II,[26] which is the most popular and used multiobjective genetic algorithm. We choose the algorithm NSGA-II because its simulation results on a number of test problems, including a five-objective, seven-constraint nonlinear problem, presented a better performance in comparison with another strategies.[26] Moreover, the constraints are managed using a multiobjective technique based on the concept of nondominance proposed by Coello−Coello.[27] The principal motivation for using an evolutionary algorithm to solve the multiobjective optimization problem formulated in this study is its population-based nature and ability to find multiple optimums simultaneously. For the reactive conventional and thermally coupled distillation systems, the multiobjective optimization problem includes, as objectives, the minimization of the total number of stages and heat duty of the sequence, and the size of the reactive section in the first column.

Also, the stochastic strategy is coupled to Aspen ONE Aspen Plus process simulator. This link allows one to obtain the rigorous Pareto front of the reactive schemes: a set of non-dominated, optimal, and rigorous designs that satisfied the purities and recoveries required. The term "non-dominated" means that there is no other design that can improve one objective without worsening another. The term "rigorous" means

Table 4. Design Parameters for Selected Optima of the Pareto Front, for Each Direct, Indirect, and Petlyuk Reactive Sequence

design parameters	direct reactive conventional sequence	direct reactive thermally coupled sequence	indirect reactive conventional sequence	indirect reactive thermally coupled sequence	Petlyuk sequence
number of stages column C1	21	16	10	22	41
number of stages column C2	7	5	15	2	21
reactive stages column C1	19	15	7	19	25
total number of stages	28	21	25	24	62
reflux ratio column C1	2.6665	2.0568	2.31	19.4216	
reflux ratio column C2	0.0607	18.2670	1.6953		42.7625
feed stage of the lauric acid	4	3	3	10	1
feed stage of the methanol	20	15	10	21	25
feed streamflow of lauric acid (lb·mol/h)	100	100	100	100	100
feed streamflow of methanol (lb·mol/h)	120	120	120	120	120
heat duty (Btu/h)	3 144 568.24	2 143 327.12	4 167 412.37	2 497 561.97	9 706 113.43
water recovered (lb·mol/h)	99.999	99.9988	99.4003	99.6056	98.4603
methanol recovered (lb·mol/h)	19.3552	18.267	19.2152	18.6912	18.9590
ester recovered (lb·mol/h)	99.9895	99.9976	99.9927	99.9999	99.3140
stage of the interconnection flow FV1		12		1	10
stage of the interconnection flow FL1		11		1	4
interconnection liquid flow FL1 (lb·mol/h)		86.2723		119.546	387.085
interconnection vapor flow FV1 (lb·mol/h)		19.8644		19.2013	280.157
feed stage to the second column C2	5		9		
pressure of the column C1 (psi)	14.7	14.7	14.7	14.7	14.7
pressure of the column C2 (psi)	14.7	14.7	14.7	14.7	14.7
column C1 diameter (ft)	1.7980	2.7212	3.6057	2.0869	2.3869
column C2 diameter (ft)	1.3070	0.6716	1.1024	0.6309	4.5091
mass fraction of water	0.9996	0.9810	0.9969	0.9870	0.9828
mass fraction of methanol	0.9964	0.9999	0.9828	0.9883	0.9814
mass fraction of ester	0.9991	0.999	0.999	0.9991	0.999
thermodynamic efficient (%)	29.86	40.6	24	46.5	11.68
CO_2 emissions (ton/year)	2432.66	1646.06	3010.28	1867.88	7796.86
total annual cost ($/year)	878,111.45	691,528.49	912,363.86	782,240.01	2,346,902.01

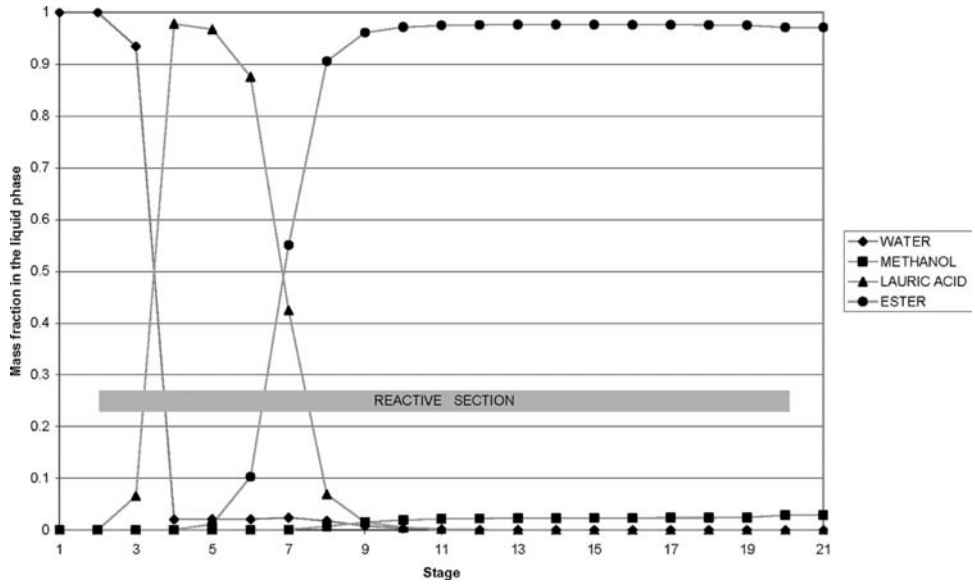

Figure 9. Composition profiles in liquid phase, column 1 of the direct reactive conventional sequence shown in Table 4.

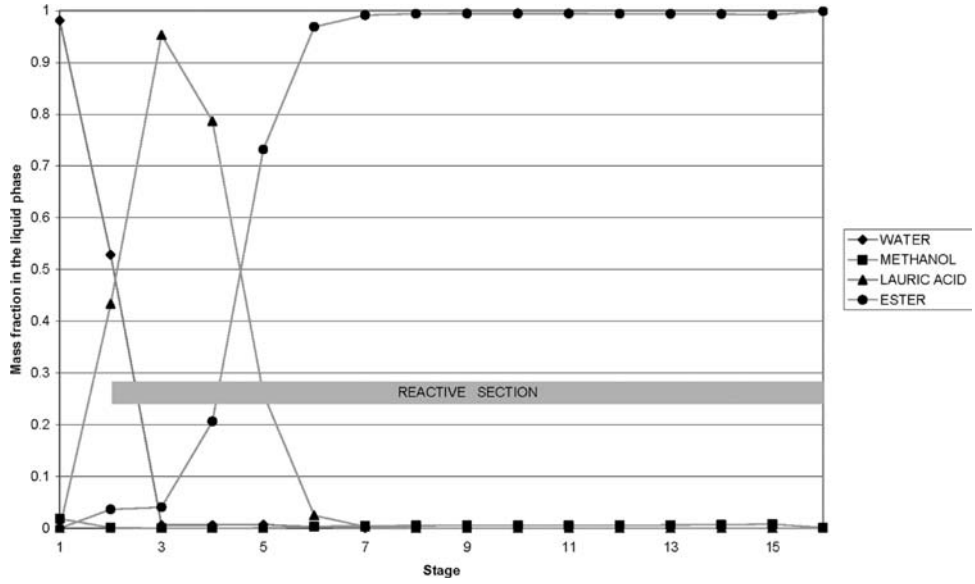

Figure 10. Composition profiles in liquid phase, column 1 of the direct reactive thermally coupled sequence shown in Table 4.

that all designs presented were obtained considering the complete set of MESH equations along with the phase equilibrium calculations, using the Radfrac module of Aspen ONE Aspen Plus. The link between Aspen Plus and the optimization procedure was realized with ActiveX Control Technology, which allows the manipulation and information exchange between applications.[23]

The multiobjective genetic algorithm works as follows. For each run, a feasible initial design of the reactive scheme is given as initial solution to the algorithm; from this initial solution, the algorithm generates N individuals to make up the initial population. The manipulated variables of each of the N individuals are sent to Aspen ONE Aspen Plus to perform the simulation; then, the algorithm retrieves, from Aspen ONE Aspen Plus, the values of objective functions and constraints for each individual. With the retrieved information, the population is divided into subpopulations according to the number of satisfied constraints; at this time, the best individuals are those that satisfy c constraints, followed by those individuals that reach $c-1$ constraints, and so on. Inside each subpopulation, the individuals are ranked on the basis of the value of the fitness function. The classification of the population makes it possible to optimize the original objective functions, but also minimizes the difference between the required and obtained constraints (recoveries and purities). At the end, a set of nondominated optimal designs of the reactive distillation arrangements is obtained. It is worthy of mention that an infinite heat duty is assigned by the algorithm to the individual where the simulation converges with errors; if the simulation does not converge, the algorithm also settles, as zero, the values of purities and recoveries. The flowchart of this stochastic approach is shown in Figure 3. For more detailed information about the algorithm, the reader is referred to the original work.[23]

For the optimization of reactive distillation sequences, we used 2000 individuals and 40 generations as parameters of the multiobjective genetic algorithm, with 0.80 and 0.05 for crossover and mutation fraction. These parameters were obtained through a tuning process. The tuning process consists of performing several runs with different number of individuals and generations, to detect the best parameters that allow

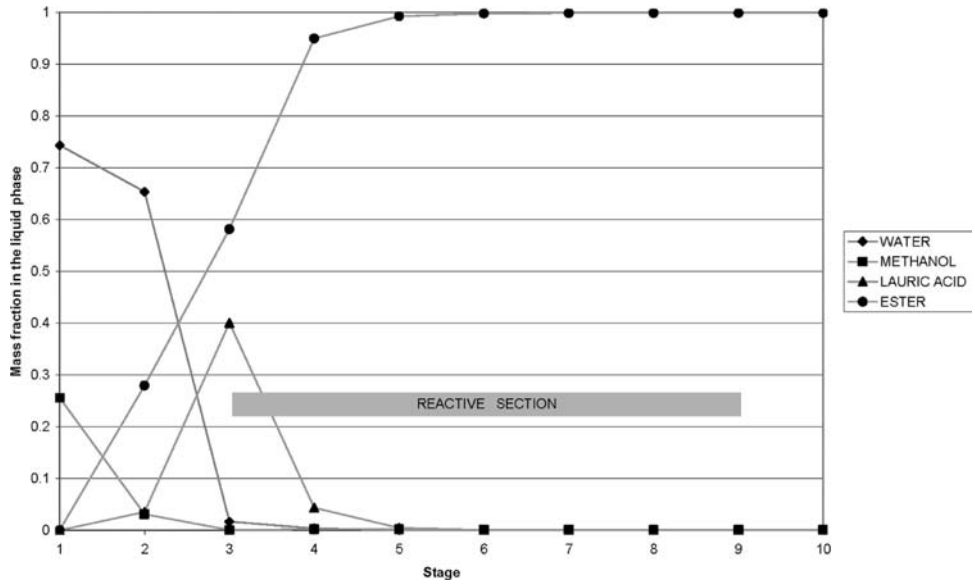

Figure 11. Composition profiles in liquid phase, column 1 of the indirect reactive conventional sequence shown in Table 4.

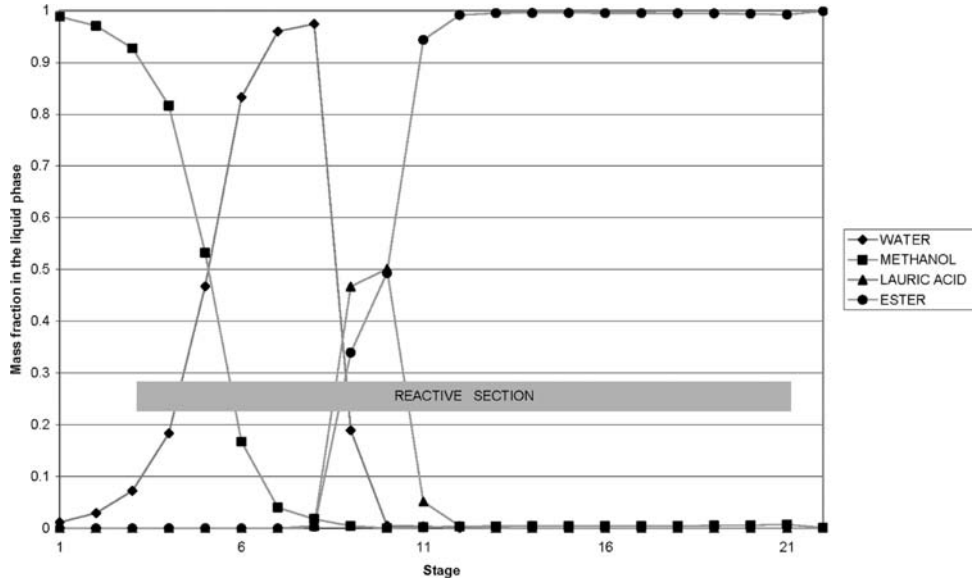

Figure 12. Composition profiles in liquid phase, column 1 of the indirect reactive thermally coupled sequence shown in Table 4.

obtaining the Pareto front. For instance, we present the convergence plot for the reactive direct conventional scheme, Figure 4. In this plot, we can see the evolution of the heat duty of the sequence as the number of generation increases, keeping a fixed number of individuals. From this graphic, we can conclude that 40 generations are enough to perform the optimization, for a given number of individuals, 2000 in this case. Similar convergence plots were generated for each reactive scheme.

The manipulated variables are varied in ranges of their values, and practically there are not restricted to certain range of values. The aim is not imposed artificial limits to them; for instance, the reflux ratio interval goes from 0.01 to 2000, while the number of stages for a column includes from 5 stages to 500.

5. Analysis of Results

In this section, we present the set of optimal designs, called Pareto front, for the conventional (direct and indirect) and thermally coupled (direct, indirect, and Petlyuk) reactive distillation sequences. It is important to recall that the Pareto front of the reactive schemes includes at least four objectives; this complicates the visualization of the results. Thereby, to visualize the results, we decide to group the objectives, showing the total heat duty as a function of the total number of stages of each reactive sequence.

Figures 5−7 show the Pareto fronts of the conventional and thermally coupled reactive distillation sequences, where objectives considered in the optimization are shown. All designs included in the Pareto fronts of conventional and thermally coupled reactive distillation sequences consider the nondominated optimal designs that satisfy the imposed constraints. Remember that an important issue is reviewing the feasibility to obtain the purity of 99.9% in mass fraction for the biodiesel (ester) in these reactive schemes. As an example, the composition profiles of one optimal design of the direct reactive thermally coupled sequence are shown in Figure 8, where we can observe that the mass fraction purity of 99.9% for the biodiesel (ester) is reached. Therefore, it is feasible to obtain biodiesel of very high purity in each of these schemes. Now,

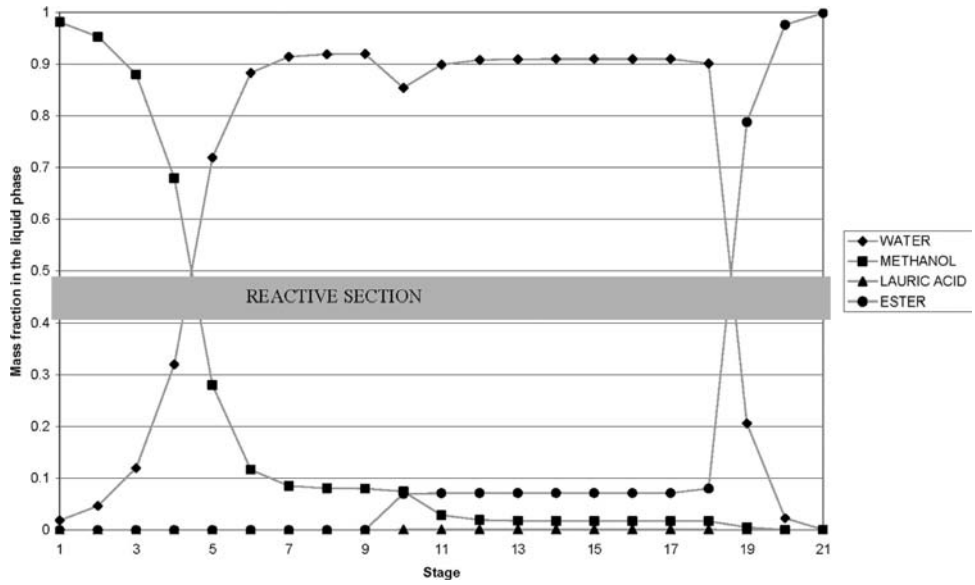

Figure 13. Composition profiles in liquid phase, column 1 of the Petlyuk sequence shown in Table 4.

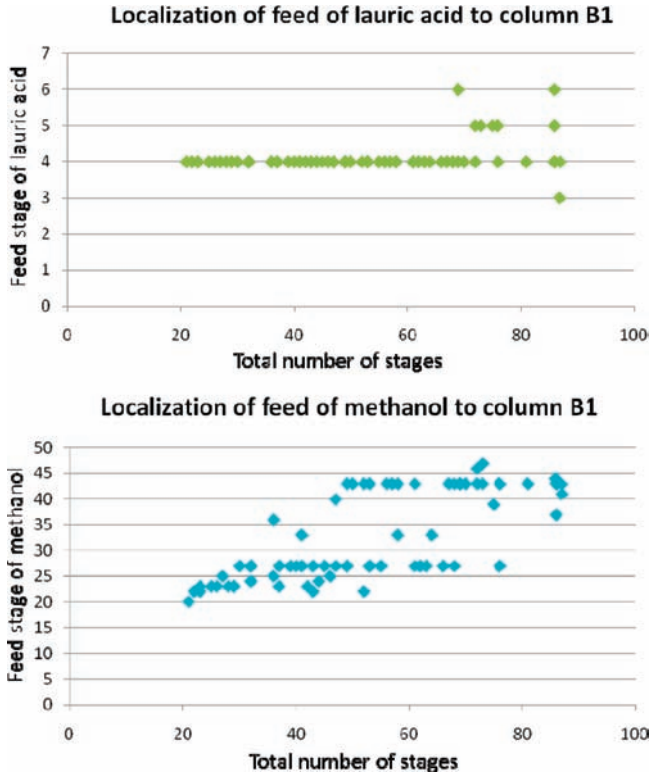

Figure 14. Feed locations of the reactives in the reactive conventional distillation sequence.

we are going to analyze the energy consumption, size of reactive sections, and other structural details of all studied schemes: direct reactive thermally coupled (STADR), direct reactive conventional (SDCR), indirect reactive thermally coupled (STAIR), direct reactive conventional (SICR), and Petlyuk (PETR).

Figure 5 shows the energy consumption of the optimal designs for STADR and SDCR sequences. It is clear that the STADR sequence has lower energy consumptions, as we expected; however, it is important to remark that these savings are not obtained by an increase in the total number of stages of the sequence, as can be seen in Figure 5. Between the STADR and SDCR sequences, the STADR has minor energy consumption, because the liquid interconnection flow acts as an additional reflux ratio, which allows improving the separation. Also, in the STADR sequence, both products are removed in the first column, a condition that favors the equilibrium of the reaction.

On the other hand, Figure 6 shows the results obtained for the indirect reactive sequences. From this figure, we can observe that the optimal designs of STAIR consume less energy than the conventional ones; even a decrease in the total number of stages of the sequence is observed. Nevertheless, the global comparison between the reactive direct and indirect sequences shows that the last ones have a small increase in energy consumption. This small increase is due to the fact that the ester is obtained in the first column with high purity, where also it is the less abundant component, with respect to the mixture of water and unreacted methanol.

Figure 7 shows the energy consumption of the designs of the Petlyuk sequence as a function of the total number of stages and the size of the reactive section. It was not expected that PETR presented the higher energetic requirements; observe how the energy consumption is more than 4 times the energy consumption of direct and indirect sequences. The increase in the energy consumption is due to the more abundant components are obtained in the side and bottom product streams; remember that the Petlyuk sequence has a good performance where the side streamflow is less abundant than the other products. From this analysis, we can expect that the Petlyuk sequence could be a good option, in terms of energy requirements, for reactions where the principal product is always more abundant than the unreacted component and byproducts, and it is not obtained in the side streamflow.

In general, the energy consumption in the SICR sequence is greater than that of the SDCR, because the reaction and separation must be performed in the first column, and the purity required for the ester is very high (99.9% in mass fraction). Therefore, the thermodynamic efficiency of the SDCR sequence is 5% higher than that of the indirect one. In the thermally coupled sequences, we can observe the opposite. The higher thermodynamic efficiency is observed in the STAIR sequence, because an easier separation (unreacted methanol from ester) is performed in the first column; in the STADR sequence, the first column performs a more difficult separation, so the thermodynamic efficiency is lower. In other words, the easier

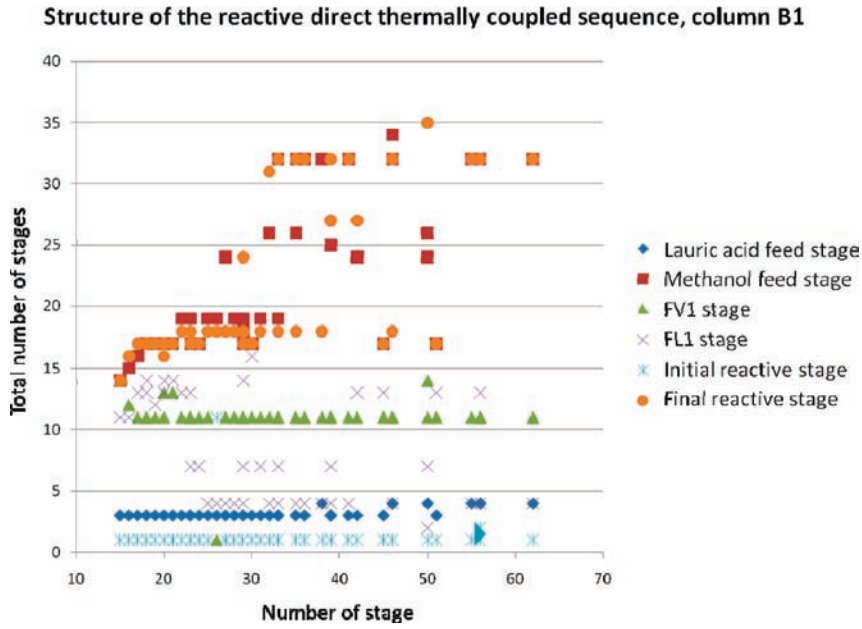

Figure 15. Variation of the input and output streams in column C1 of the direct reactive thermally coupled sequences of the Pareto front.

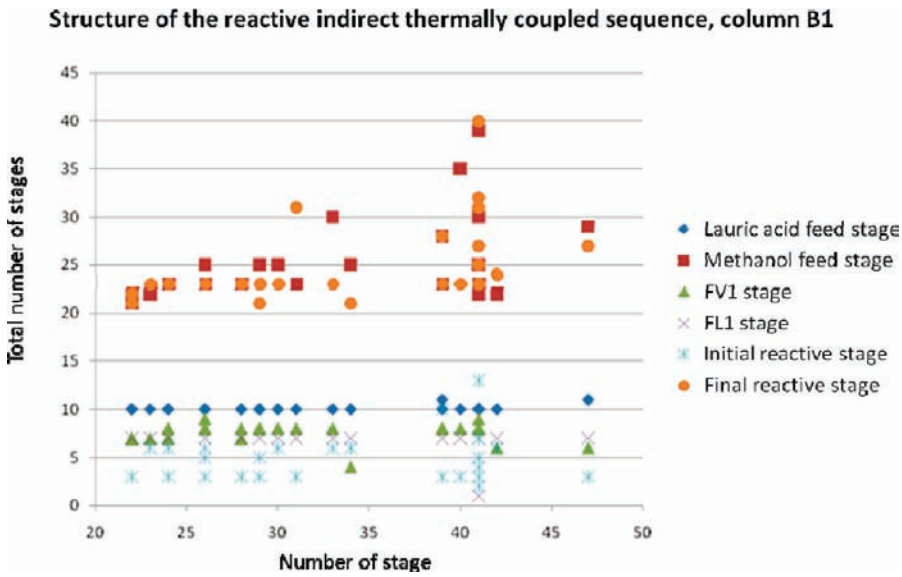

Figure 16. Variation of the input and output streams in column C1 of the indirect reactive thermally coupled sequences of the Pareto front.

separation must be performed in the first column, and the difficult in the next ones; this issue has been observed also for nonreactive separations.[23]

Table 4 shows some selected designs of Pareto fronts of all considered sequences. Remember that the reactive section is just presented in the first column, because the equilibrium reaction is favored if the products are removed from the column as they are produced. From Table 4, we observe that the reactive section size in the first column includes almost the entire column; excepting the Petlyuk sequence, this is a common characteristic of all schemes, Figures 9−13. Note that the feed of the reactants is located at the ends of the column, allowing better interaction between them. Also, the composition profiles indicated in Figures 9−13 can be used to understand the distribution of reactants and products in the product streams. For instance, in Figure 9, it can be seen that in the reactive column of the SDCR, the water is obtained as distillate, and the bottoms product is a mixture of ester and methanol that are separated in the next column. A similar analysis can be done for the STADR; the composition profiles indicated in Figure 10 show that in the reactive distillation column, the water is obtained as distillate, while the ester is obtained in the bottoms product.

In the case of the indirect sequences, Figures 11 and 12 indicate that the ester is obtained as bottoms product. It is important to mention that for the SICR an additional distillation column is required to separate the mixture of methanol and water. When the composition profiles of the STAIR are analyzed, it can be noted that the water is removed as distillate in the reactive distillation column and the methanol is recovered in the side stripper.

For the reactive Petlyuk distillation column (Figure 13), the composition profiles indicate that the purity of the ester can be obtained, but with high energy requirements, in comparison with the configurations with side equipments.

The location of the feeding of the reactive agents to the sequences is described below. In all sequences, the location of the feed stage where lauric acid is introduced to column C1

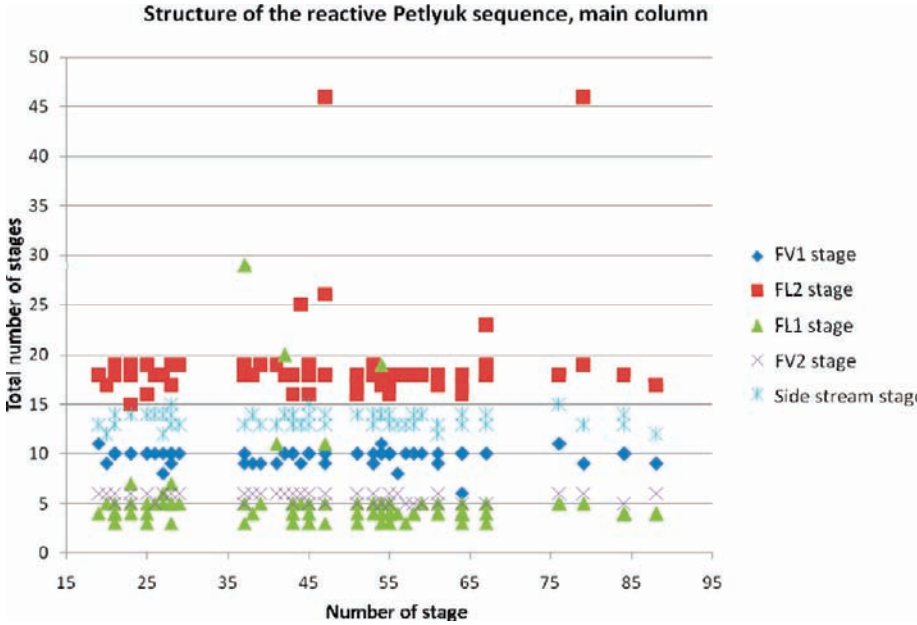

Figure 17. Variation of the input and output streams in the main column of the Petlyuk sequences of the Pareto front.

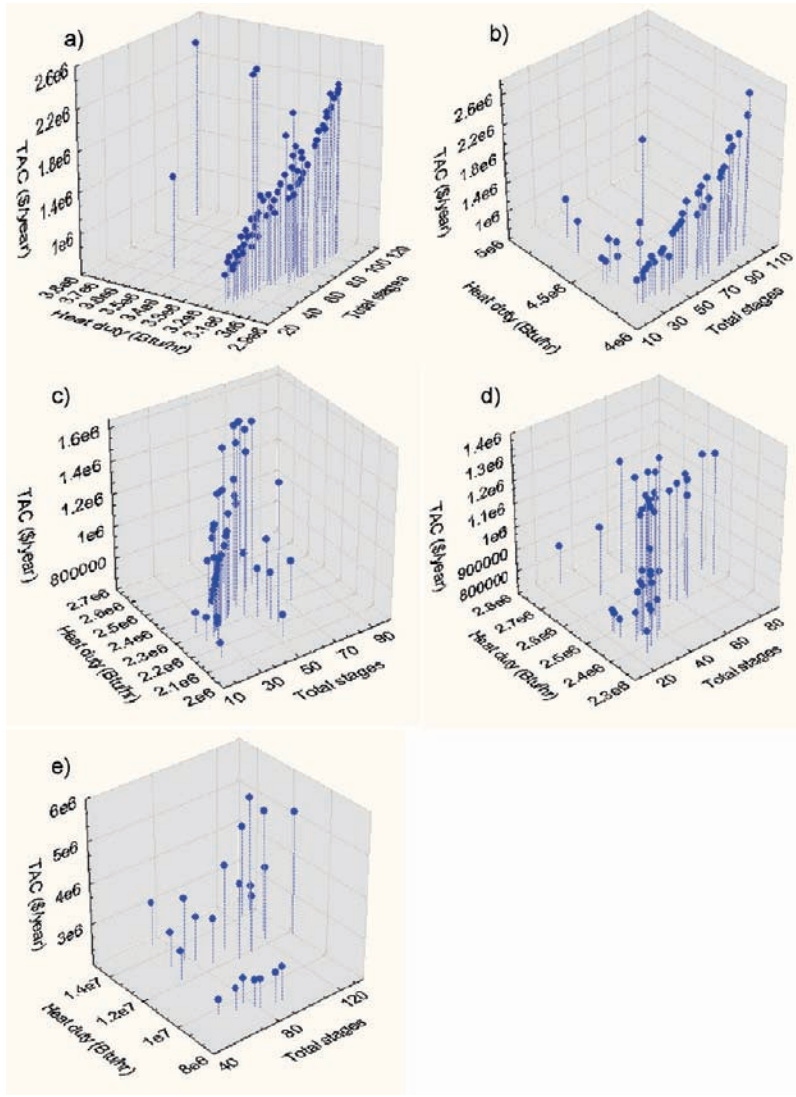

Figure 18. Total annual cost as a function of heat duty and total number of stages of conventional reactive direct (a) and indirect (b), along with the thermally coupled reactive direct (c), indirect (d), and Petlyuk (e) sequences.

practically remains unchanged in all designs of the Pareto front, Figure 14. On the other hand, the stage where methanol is introduced varies considerably, according to the total number of stages of column C1. In this way, the Pareto front is integrated. The observed behavior is presented in all the studied sequences, which suggests that the location of lauric acid is not changed because it is the limiting reactive, while methanol can be moved due to it being the excess reactive. Nevertheless, further research is needed to confirm this finding.

The structure of the thermally coupled reactive sequences exhibits interesting behavior. Figure 15 shows the variation of the structure of the first column (C1) of the direct reactive thermally coupled sequence. From this figure, we can observe how the location of the interconnection flows, the initial reactive stage, and the location of the feed of lauric acid practically remain unchanged. Here, the Pareto front is integrated with the variation in the size of the reactive section and, of course, the location of the feed stage of methanol. A similar behavior is observed in the indirect reactive thermally coupled and Petlyuk sequences, Figures 16 and 17.

The total annual costs as a function of the heat duty and total number of stages for all studied sequences are presented in Figure 18. From this figure, we observe the diversity in the Pareto front, which includes a considerable amount of optimal and nondominated designs with different design parameters, but all satisfying the imposed constraints, as purities and recoveries.

Regarding environmental aspects, Kencse and Mizsey[28] have reported that, in fact, gas emissions are directly linked to energy consumption because, in the chemical industry, the energy required in distillation is obtained from crude oil. As a result, reductions in energy consumption can be translated into reductions in carbon dioxide emissions. In other words, carbon dioxide emissions can increase significantly when the operational conditions are different than those corresponding to the optimum. This point is important, because in terms of control and operational aspects, it has been reported[29] that the control properties of coupled schemes can be improved when the operational conditions fall outside the optimum. This is significant because, in the selection of operational conditions, the engineer must take into account the fact that savings in carbon dioxide emissions can be achieved with additional efforts in the control system.

6. Conclusions

This study introduces the application of a multiobjective optimization approach for the design of reactive distillation sequences with thermal coupling. The esterification of methanol and lauric acid using sulfuric acid, as catalyst, was studied in direct and indirect reactive sequences, both conventional and thermally coupled. The optimal designs were obtained through a multiobjective genetic algorithm with constraints, which is coupled to Aspen ONE Aspen Plus. The results show that obtaining the ester with a purity of 99.9% is feasible in conventional and thermally coupled distillation sequences. However, lower energy consumptions, and lower CO_2 emissions, are observed in the thermally coupled sequences. The direct reactive sequences require less energy when the product of interest, ester in this case, is the most abundant component, because the separation task is easier and the energy requirements are lower. These findings are important because, depending on the type of reaction and byproducts involved, we know the better sequence beforehand. For instance, from this analysis, we can expect that the Petlyuk sequence could be a good option, in terms of energy requirements, for reactions where the principal product is always more abundant than the unreacted component and byproducts. Also, an important issue is the role that the limiting and excess reactives play in the integration of the Pareto front.

Acknowledgment

We acknowledge the financial support provided by Universidad de Guanajuato, CONACyT, through project 84552, and CONCyTEG (Mexico).

Literature Cited

(1) Stankiewicz, A. I.; Moulijn, J. A. Process Intensification: Transforming Chemical Engineering. *Chem. Eng. Prog.* **2000**, 22–34.

(2) Moulijn, J. A.; Stankiewicz, A.; Grievink, J.; Gorak, A. Process Intensification and Process Systems Engineering: A Friendly Symbiosis. *Comput. Chem. Eng.* **2008**, *32*, 3–11.

(3) Harmsen, G. J. Reactive Distillation: The Front-Runner of Industrial Process Intensification: A full Review of Commercial Applications, Research, Scale-up, Design and Operation. *Comput. Chem. Eng.* **2007**, *46*, 774–780.

(4) Doherty, M. F.; Buzad, G. Reactive Distillation by Design. *Chem. Eng. Res. Des.* **1992**, *70*, 448.

(5) Ciric, A. R.; Gu, D. Synthesis of Nonequilibrium Reactive Distillation Processes by MINLP Optimization. *AIChE J.* **1994**, *40*, 1479.

(6) Viswanathan, J.; Grossmann, I. E. Combined-Penalty Function and Outer-Approximation Method for MINLP Optimization. *Comput. Chem. Eng.* **1990**, *14*, 769.

(7) Viswanathan, J.; Grossmann, I. E. Optimal Feed Locations and Number of Trays for Distillation Columns with Multiple Feeds. *Ind. Eng. Chem. Res.* **1993**, *32*, 2942.

(8) Jackson, J. R.; Grossmann, I. E. A Disjunctive Programming Approach for the Optimal Design of Reactive Distillation Columns. *Comput. Chem. Eng.* **2001**, *25*, 1661.

(9) Yeomans, H.; Grossmann, I. E. Disjunctive Programming Models for the Optimal Design of Distillation Columns and Separation Sequences. *Ind. Eng. Chem. Res.* **2000**, *39*, 1637.

(10) Triantafyllou, C.; Smith, R. The Design and Optimization of Fully Thermally Coupled Distillation Columns. *Chem. Eng. Res. Des.* **1992**, *70*, 118.

(11) Hernández, S.; Jiménez, A. Design of Optimal Thermally-coupled Distillation Systems Using a Dynamic Model. *Chem. Eng. Res. Des.* **1996**, *74*, 357.

(12) Hernández, S.; Jiménez, A. Design of Energy-Efficient Petlyuk Systems. *Comput. Chem. Eng.* **1999**, *23*, 1005.

(13) Dünnebier, G.; Pantelides, C. Optimal Design of Thermally Coupled Distillation Columns. *Ind. Eng. Chem. Res.* **1999**, *38*, 162.

(14) Emtir, M.; Mizsey, P.; Rev, E.; Fonyo, Z. Economic and Controllability Investigation and Comparison of Energy-Integrated Distillation Schemes. *Chem. Biochem. Eng. Q.* **2003**, *17*, 31.

(15) Olujic, Z.; Kaibel, B.; Jansen, H.; Rietfort, T.; Zich, E.; Frey, G. Distillation Column Internals/Configurations for Process Intensification. *Chem. Biochem. Eng. Q.* **2003**, *17*, 301.

(16) Hernández, S.; Segovia-Hernández, J. G.; Rico-Ramírez, V. Thermodynamically Equivalent Distillation Schemes to the Petlyuk Column for Ternary Mixtures. *Energy* **2006**, *31*, 1840.

(17) Abad-Zarate, E. F.; Segovia-Hernández, J. G.; Hernández, S.; Uribe-Ramírez, A. R. A Short Note on Steady State Behavior of a Petlyuk Distillation Column by Using a Nonequilibrium Stage Model. *Can. J. Chem. Eng.* **2006**, *84*, 381.

(18) Errico, M.; Rong, B. G.; Tola, G.; Turunen, I. Process Intensification for the Retrofit of a Multicomponent Distillation Plant-An Industrial Case Study. *Ind. Eng. Chem. Res.* **2008**, *47*, 1975.

(19) Barroso-Muñoz, F. O.; Hernández, S.; Segovia-Hernández, J. G.; Hernández-Escoto, H.; Aguilera-Alvarado, A. F. Thermally Coupled Distillation Systems: Study of an Energy - Efficient Reactive Case. *Chem. Biochem. Eng. Q.* **2007**, *21*, 115.

(20) Wang, S. J.; Wong, D. S. H.; Yu, S. W. Design and Control of Transesterification Reactive Distillation with Thermal Coupling. *Comput. Chem. Eng.* **2008**, *32*, 3030.

(21) Hernández, S.; Sandoval-Vergara, R.; Barroso-Muñoz, O. F.; Murrieta-Dueñas, R.; Hernández-Escoto, H.; Segovia-Hernández, J. G.; Rico-Ramírez, V. Reactive Divided Wall Distillation Columns: Dynamic Simulation and Implementation in a Pilot Plant. *Chem. Eng. Process.: Process Intensif.* **2009**, *48*, 250.

(22) Kiss, A. A.; Pragt, J. J.; Van Strien, J. G. Reactive Dividing-Wall Columns−How to Get More with Less Resources? *Chem. Eng. Commun.* **2009**, *196*, 1366.

(23) Gutiérrez-Antonio, C.; Briones-Ramírez, A. Pareto Front of Ideal Petlyuk Sequences Using a Multiobjective Genetic Algorithm with Constraints. *Comput. Chem. Eng.* **2009**, *33*, 454.

(24) Omota, F.; Dimian, A. C.; Bliek, A. Fatty Acid Esterification by Reactive Distillation: Part 2−Kinetics-Based Design for Sulphated Zirconia Catalysts. *Chem. Eng. Sci.* **2003**, *58*, 3159.

(25) Steinigeweg, S.; Gmehling, J. Esterification of a Fatty Acid by Reactive Distillation. *Ind. Eng. Chem. Res.* **2003**, *42*, 3612.

(26) Deb, K.; Agrawal, S.; Pratap, A.; Meyarivan, T. A fast elitist non-dominated sorting genetic algorithm for multiobjective-optimization: NSGA-II. KanGAL report 200001; Indian Institute of Technology: Kanpur, India, 2000.

(27) Coello-Coello, C. A. Constraint-Handling Using and Evolutionary Multiobjective Optimization Technique. *Civil Eng. Environ. Syst.* **2000**, *17*, 319.

(28) Kencse, H.; Mizsey, P. Methodology for the Design and Evaluation of Distillation Systems: Exergy Analysis, Economic Features and GHG Emissions. *AIChE J.* **2009**, in press.

(29) Serra, M.; Spuña, A.; Puigjaner, L. Controllability of Different Multicomponent Distillation Arrangements. *Ind. Eng. Chem. Res.* **2003**, *42*, 1773–1782.

Received for review June 15, 2010
Revised manuscript received November 23, 2010
Accepted November 24, 2010

IE101290T